Large sensitive-area NbN nanowire superconducting single-photon detectors fabricated on single-crystal MgO substrates

Shigehito Miki,[1,a)] Mikio Fujiwara,[1] Masahide Sasaki,[1] Burm Baek,[2] Aaron J. Miller,[4] Robert H. Hadfield,[3] Sae Woo Nam,[2] and Zhen Wang[1]
[1]*National Institute of Information and Communications Technology, 4-2-1 Nukui-Kitamachi, Koganei, Tokyo 184-8795, Japan*
[2]*National Institute of Standards and Technology, 325 Broadway, Boulder, Colorado 80305, USA*
[3]*School of Engineering and Physical Sciences, Heriot-Watt University, Edinburgh, EH14 4AS, United Kingdom*
[4]*Department of Physics and Astronomy, Albion College 611 East Porter Street, Albion, Michigan 49224, USA*

(Received 7 September 2007; accepted 28 January 2008; published online 15 February 2008)

We report on the performance of large area NbN nanowire superconducting single-photon detectors (SSPDs). 20×20 μm^2 area SSPDs with 80 and 100 nm linewidths and 50% fill factor were fabricated in 4-nm-thick NbN films grown on single-crystal MgO substrates. The high quality of the devices was verified by electrical and optical testing and compares favorably to measurements of 10×10 μm^2 area SSPDs. Measurements of kinetic inductance versus bias current indicate that the constriction density is low. The fiber-coupled detection efficiency of the devices was 0.4%–3.5% at 100 Hz dark count rate. © *2008 American Institute of Physics*. [DOI: 10.1063/1.2870099]

Niobium nitride (NbN) nanowire superconducting single-photon detectors (SSPDs) have recently attracted much attention in the fields of quantum information processing and sensing because of their infrared single-photon sensitivity, with low dark count rates, excellent timing resolution, and short recovery times.[1–3] NbN ultrathin films are used for SSPDs because they have relatively high transition temperature (T_c) even at a thickness of several nanometers, allowing the intrinsically fast energy relaxation of ~30 ps (Ref. 4) to be exploited with high photon sensitivity. SSPDs have been successfully employed in quantum key distribution (QKD) experiments, boosting both transmission distances and key generation rates rate.[5,6] However, further improvements in device performance are highly desirable and will broaden the impact of SSPDs in QKD and other quantum information processing applications. In particular, significant effort is being put into increasing the detection efficiency (DE) and continuous photon counting rate.

A primary factor limiting the counting rate is the large kinetic inductance (KI) of the nanowire which determines the device recovery time after photon absorption.[7,8] Reducing the active detector area is a natural way to reduce the KI. However, a new speed limitation due to latching behavior has been pointed out for smaller devices.[9] In order to circumvent such limitations of a single device, many detectors will have to be used parallel[10] or as an independently addressable array. SSPD arrays may also enable spatial and pseudo-photon-number resolution to be achieved.[11,12]

Improving device DE is essential for realizing various quantum information processing protocols which require coincident photon detection by multiple detectors. The DE is determined by the intrinsic photoabsorption coefficient of, and the effective optical coupling coefficient to the active area. The main concern in packaging fiber-coupled detectors is to improve the latter. However, a further limiting factor specific to SSPDs is the constriction of the nanowire caused by a defect in the superconducting film or introduced during nanofabrication.[13] Because the critical current of the entire wire is limited by the smallest constriction, the critical current density elsewhere in the wire remains low, reducing the DE.

Thus, to produce high performance SSPDs or to realize a multiformat array it is important to develop the fabrication technology that produces devices with few constrictions and small KI over large area. Such development requires careful selection and control of deposition methods and conditions. For example, NbN thin films prepared by rf sputtering at an ambient substrate temperature include granular or columnar void structures and show high resistivity ranging from 150 to over 10^4 $\mu\Omega$ cm, and a large KI.[14]

We have developed a method for growing 4.2-nm-thick NbN epitaxial films directly on a single crystal MgO substrate by reactive dc magnetron sputtering at room temperature. Epitaxial growth directly on the substrate has been confirmed by transmission electron microscopy.[15] These films show $T_C\sim12$ K and a lower resistivity at 20 K ($\rho_{20\ K}$) ~120 $\mu\Omega$ cm even for the thin films of 4.2 nm thickness,[15,16] which should yield a high uniformity nanowire (i.e., with a low probability of constrictions) over large area. Using these high quality films, we fabricated 80- and 100-nm-wide meander lines covering a relatively large area of 20×20 μm^2 with a filling factor of 50%. The fabrication process and dc characteristics of SSPDs are described in detail elsewhere.[17]

A scanning electron micrograph (SEM) of our SSPD is shown in Fig. 1(a). The meander pattern was embedded in a coplanar waveguide structure fabricated from 150-nm-thick NbN films. Figures 1(b) and 1(c) show histograms of measured values of the sheet resistance at 20 K ($R_{sheet,20\ K}$) and critical current density (J_C), respectively, of our 80- and 100-nm-wide meanders in a film grown under identical conditions on an MgO substrate. A total of five (seven) samples of 80-(100-) nm-wide meanders were measured. $R_{sheet,20\ K}$ and J_C were converted from the measured resistance at 20 K

[a)]Electronic mail: s-miki@nict.go.jp.

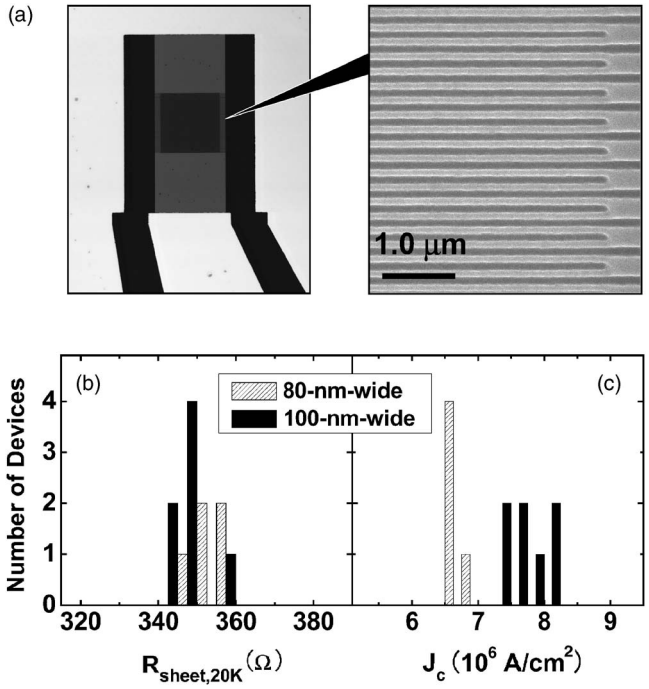

FIG. 1. (a) Scanning electron micrograph (SEM) of our SSPD device. The meander pattern of 100-nm-wide nanowire covering 20×20 μm^2 area was embedded in a 50 Ω coplanar waveguide structure fabricated from 150-nm-thick NbN films. Histograms of (b) sheet resistance and (c) J_C of our five (seven) SSPDs with 80-(100-) nm-wide meanders of 4.2-nm-thick NbN films on a common MgO substrate.

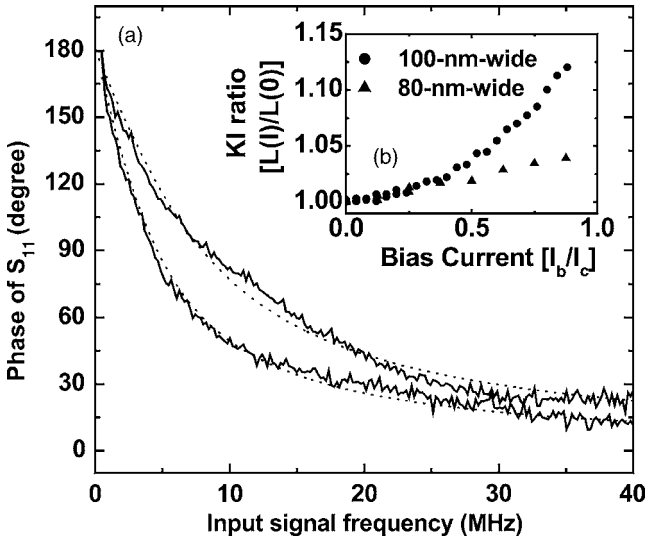

FIG. 2. (a) The phase of S_{11} as a function of frequency for two devices: 100-nm-wide nanowire device (total nanowire length was 2000 μm) and 80-nm-wide nanowire device (total nanowire length was 2500 μm). The solid lines are measured data and the dotted lines are curves fitted using the expression of arg $[(j\omega L-50\ \Omega)/(j\omega L+50\ \Omega)]$. (b) The bias current dependencies of L_k^{device}. The L_k^{device} and bias current are scaled by $L_k^{\text{device}}(I_b/I_C=0)$ and I_C, respectively.

$(R_{20\ \mathrm{K}})$ and the critical current (I_C) of the meanders by using the design geometry. As shown in Fig. 1(b), the $R_{\text{sheet,20 K}}$ values were almost the same regardless of different samples and designs, indicating the meanders were reproducibly fabricated as designed. On the other hand, the J_C of the devices, which will be limited by any local defects anywhere in the nanowire, were smaller for 80-nm-wide meanders than for 100-nm-wide meanders. This discrepancy in J_C indicates that the 80-nm-wide meanders have more constrictions than wider meanders; this is expected because the narrow meander is 1.25 times longer. However, the variation among like-width meanders are within $\pm5\%$, implying the high reproducibility of patterning.

We evaluated the KI of our SSPDs using both theoretical prediction and actual measurement. Theoretically, the KI per square thickness $\langle L_k\rangle$ is given by $\mu_0\lambda^2$, where μ_0 is the permeability of free space and λ is penetration depth. The value of λ is predicted from the expressions given by Orlando *et al.*[18] by substituting T_c and $\rho_{20\ \mathrm{K}}$ of our device.[16] This prediction results in $\langle L_k\rangle=119.7$ *p*H nm.

We also measured the KI of the devices, $L_k^{\text{device}}(=\mu_0\lambda^2 l/d)$ with the line length l and thickness d, by observing the phase of the reflection coefficient S_{11}. Because the device impedance has no resistive component when in the superconducting state, S_{11} of the device is expressed as $(j\omega L-50\ \Omega)/(i\omega L+50\ \Omega)$. The L_k^{device} is obtained by fitting the data to this expression with L as the free parameter. Figure 2(a) shows the typical phase of S_{11} as a function of frequency for the two kinds of devices at zero bias current. As shown in the figure, $L_k^{\text{device}}=1.73\mu$H for a typical 80-nm-wide device and $L_k^{\text{device}}=1.00$ μH for a typical 100-nm-wide device, which correspond to 20 and 34.6 ns recovery times $(L_k^{\text{device}}/50\ \Omega)$, respectively. The $\langle L_k^{\text{device}}\rangle$ values are 232 and 210 pH nm for 80- and 100-nm-wide meanders. These values are similar or lower than those reported previously[7,19] in spite of the fact that our devices are four times larger, which may be due to differences in the properties of the basic NbN films. The measured KI values for our devices are approximately a factor of two larger than the values predicted from the simple theory described above. They are expected to approach the theoretical values with further improvements to the nanowire uniformity.

Figure 2(b) shows the bias current dependencies of L_k^{device}. The KI and the bias current I_b are scaled by the value $L_k^{\text{device}}(I_b/I_C=0)$ and the critical current I_c, respectively. According to Ref. 13, the L_k^{device} should increase monotonically with increasing I_b and reach about 120% of $L_k^{\text{device}}(0)$ at $I_b/I_C=0.9$ when there is no constriction. On the other hand, this upturn in L_k^{device} is suppressed in imperfect devices. The degree of constriction can be estimated by this relation.[13] For our SSPDs, $L_k^{\text{device}}(0.9)/L_k^{\text{device}}(0)=4\%$ and 12% for the 80- and 100-nm-wide devices. In Ref. 13 the maximum upturn reported in a 3×3.3 μm^2, 90 nm linewidth device at 1.8 K (40 times smaller than our devices) was 22% from a sample of >100 devices; in Ref. 19 an upturn of 8% was reported in a 10×10 μm^2, 100 nm linewidth device at 4 K. Our results indicate that we have achieved similar or lower defect densities to typical good quality 10×10 μm^2 devices (as reported in Ref. 19), with four times the device area.

Optical testing was performed on multiple fiber-coupled SSPDs in a Gifford–MacMahon closed-cycle refrigerator system.[8] We measured the DE of our whole system including the optical coupling efficiency, referred hereafter to as the system DE. The incident photons are introduced through a single mode telecommunications fiber (9 μm core diameter) to the SSPD. Prior to cooling, the end of a fiber is accurately aligned to the center of each device with a gap of 50–100 μm.[20] The packaged device is cooled to 2.4–2.6 K with ~20 mK thermal fluctuation at the operating temperature. The output port from the nanowire was connected to a

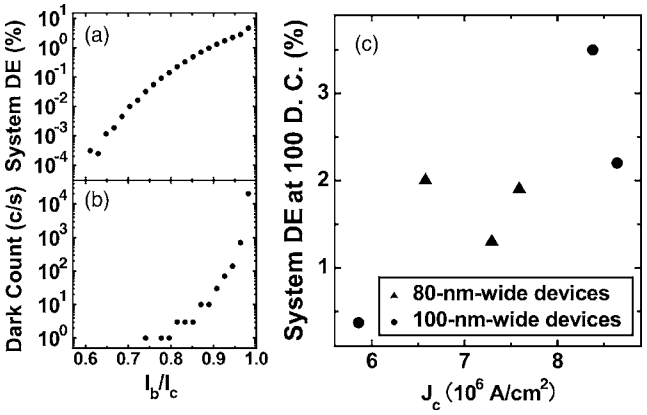

FIG. 3. (a) The system DE and (b) dark count of a typical 80-nm-wide device as a function of I_b/I_c. (c) The system DE for three devices with 80-nm-width and three with 100-nm-width at a dark count rate of 100 Hz.

parallel shunt resistance (50 Ω) and a bias tee at room temperature through a 50 Ω coaxial cable. The shunt resistance is to prevent latching of the biased device and is placed outside of the cryocooler to allow back reflections to be attenuated. The device is current-biased via the dc arm of the bias tee. The output signal from the ac arm of the bias tee is amplified using a series of two low noise amplifiers (RF bay Inc., LNA 500 and LNA 1000), and then observed by a pulse counter or an oscilloscope. A 1550 nm wavelength continuous laser diode with power of 1 mW is used for the input photon source, and is heavily attenuated to $-70\sim-100$ dBm at the input connector of the cryostat by attenuators so that the count rate is in the range of 10 kHz–1 MHz. A polarization controller is inserted in front of the cryocooler optical input to control the polarization properties of incident photons to match the polarization sensitivity (maximizing the DE) of each device.

Figures 3(a) and 3(b) show the system DE and the dark count rate of a typical 80-nm-wide device as a function of I_b/I_C. Although the system DE increases as the I_b approaches to I_C, there is no saturation region. This is a further indication that constrictions in the nanowire limit the DE. Figure 3(c) shows the system DEs as a function of J_C for three devices with 80-nm-width and three with 100-nm-width at a dark count rate of 100 Hz. A tendency can be seen that a higher J_C shows a higher system DE; this implies that the optical coupling efficiency is almost the same for all six devices and the constrictions in nanowire limit the system DE, as described in Ref. 13. The system DE (at 100 Hz dark count rate) of five devices among the six measured exceeds 1%, and the best system DE attained was 3.5%. The intrinsic DE of the NbN nanowires seems much higher according to the result of Ref. 13 giving us confidence that careful optimization of optical alignment will result in further increases to the system DE.

In conclusion, we have reported the performance of epitaxially grown NbN nanowire SSPDs on a MgO substrate with a large 20×20 μm^2 meander area. In spite of the increased area as compared to other previously reported devices, we succeeded in fabricating SSPDs with fewer constrictions and lower KIs implying a minimum 28 MHz continuous counting rate with relatively high DEs of 0.4%–3.5% at a nominal dark count rate of 100 Hz. These new devices will enable improved performance in QKD and other photon counting applications. Furthermore, we have now demonstrated large active area devices—a crucial step toward the fabrication of future large area arrays.

[1] G. Gol'tsman, O. Okunev, G. Chulkova, A. Lipatov, A. Semenov, K. Smirnov, B. Voronov, A. Dzardanov, C. Williams, and R. Sobolewski, Appl. Phys. Lett. **79**, 705 (2001).
[2] A. Korneev, V. Matvienko, O. Minaeva, I. Milostnaya, I. Rubtsova, G. Chulkova, K. Smirnov, V. Voronov, G. Gol'tsman, W. Slysz, A. Pearlman, A. Verevkin, and R. Sobolewski, IEEE Trans. Appl. Supercond. **15**, 571 (2005).
[3] K. M. Rosfjord, J. K. W. Yang, E. A. Dauler, A. J. Kerman, V. Anant, B. M. Boronov, G. N. Gol″tsman, and K. K. Berggren, Opt. Express **14**, 527 (2006).
[4] K. S. Il'in, M. Lindgren, M. Currie, A. D. Semenov, G. N. Gol'tsman, R. Sobolewski, S. I. Cherednichenko, and E. M. Gershenzon, Appl. Phys. Lett. **76**, 2752 (2000).
[5] R. H. Hadfield, J. L. Habif, J. Schlafer, R. E. Schwall, and S. Nam, Appl. Phys. Lett. **89**, 241129 (2006).
[6] H. Takesue, S. Nam, Q. Zhang, R. H. Hadfield, T. Honjo, K. Tamaki, and Y. Yamamoto, Nat. Photonics **1**, 343 (2007).
[7] A. J. Kerman, E. A. Dauler, W. E. Keicher, J. K. W. Yang, K. Berggren, G. Gol'tsman, and B. Voronov, Appl. Phys. Lett. **88**, 111116 (2006).
[8] R. H. Hadfield, A. J. Miller, S. W. Nam, R. L. Kautz, and R. E. Schwall, Appl. Phys. Lett. **87**, 203505 (2005).
[9] J. K. W. Yang, A. J. Kerman, E. A. Dauler, V. Anant, K. M. Rosfjord, and K. K. Berggren, IEEE Trans, IEEE Trans. Appl. Supercond. **17**, 581 (2007).
[10] M. Ejrnaes, R. Cristiano, O. Quaranta, S. Pagano, A. Gaggero, F. Mattioli, R. Leoni, B. Voronov, and G. Gol'tsman, Appl. Phys. Lett. **91**, 262509 (2007).
[11] E. A. Dauler, B. S. Robinson, A. J. Kerman, J. K. W. Yang, K. M. Rosfjord, V. Anant, B. Voronov, G. Gol'tsman, and K. K. Bergren, IEEE Trans. Appl. Supercond. **17**, 279 (2007).
[12] G. Gol'tsman, O. Minaeva, A. Korneev, M. Tarkhov, I. Rubtsova, A. Divochiy, I. Milostnaya, G. Chulkova, N. Kaurova, B. Voronov, D. Pan, J. Kitaygorsky, A. Cross, A. Pearlman, I. Komissarov, W. Slysz, M. Wegrzecki, P. Grabiec, and R. Sobolewski, IEEE Trans. Appl. Supercond. **17**, 246 (2007).
[13] A. J. Kerman, E. A. Dauler, J. K. W. Yang, K. M. Rosfjord, V. Anant, K. Berggren, G. N. Gol'tsman, and B. M. Voronov, Appl. Phys. Lett. **90**, 101110 (2007).
[14] J. Cukauskas, J. Appl. Phys. **54**, 1013 (1983).
[15] S. Miki, Y. Uzawa, A. Kawakami, and Z. Wang, Electron. Commun. Jpn. **85**, 77 (2002).
[16] Z. Wang, A. Kawakami, Y. Uzawa, and B. Komiyama, J. Appl. Phys. **79**, 7837 (1996).
[17] S. Miki, M. Fujiwara, M. Sasaki, and Z. Wang, IEEE Trans. Appl. Supercond. **17**, 285 (2007).
[18] T. P. Orlando, E. J. McNiffJr., and S. Foner, Phys. Rev. B **19**, 4545 (1979).
[19] R. H. Hadfield, P. A. Dalgarno, J. A. O'Connor, E. Ramsay, R. J. Warburton, E. J. Gansen, B. Baek, M. J. Stevens, R. P. Mirin, and S. W. Nam, Appl. Phys. Lett. **91**, 241108 (2007).
[20] R. H. Hadfield, M. J. Stevens, S. S. Gruber, A. J. Miller, R. E. Schwall, R. P. Mirin, and S. W. Nam, Opt. Express **13**, 26 (2005).